MEMORANDUM REPORT BRL-MR-3757

BRL

A MULTIDRIVER SHOCK TUBE MODEL
OF A LARGE BLAST SIMULATOR

EDMUND J. GION

MAY 1989

U.S. ARMY LABORATORY COMMAND

BALLISTIC RESEARCH LABORATORY
ABERDEEN PROVING GROUND, MARYLAND

DESTRUCTION NOTICE

REPORT DOCUMENTATION PAGE

Form Approved
OMB No. 0704-0188

1a. REPORT SECURITY CLASSIFICATION UNCLASSIFIED	1b. RESTRICTIVE MARKINGS

2a. SECURITY CLASSIFICATION AUTHORITY	3. DISTRIBUTION / AVAILABILITY OF REPORT
2b. DECLASSIFICATION / DOWNGRADING SCHEDULE	Approved for public release; distribution is unlimited.

4. PERFORMING ORGANIZATION REPORT NUMBER(S) BRL-MR- 3757	5. MONITORING ORGANIZATION REPORT NUMBER(S)

6a. NAME OF PERFORMING ORGANIZATION U. S. Army Ballistic Research Laboratory (BRL)	6b. OFFICE SYMBOL (If applicable) SLCBR-TB-B	7a. NAME OF MONITORING ORGANIZATION

6c. ADDRESS (City, State, and ZIP Code) Aberdeen Proving Ground, MD 21005-5066	7b. ADDRESS (City, State, and ZIP Code)

8a. NAME OF FUNDING / SPONSORING ORGANIZATION	8b. OFFICE SYMBOL (If applicable)	9. PROCUREMENT INSTRUMENT IDENTIFICATION NUMBER

8c. ADDRESS (City, State, and ZIP Code)	10. SOURCE OF FUNDING NUMBERS			
	PROGRAM ELEMENT NO.	PROJECT NO.	TASK NO.	WORK UNIT ACCESSION NO.

11. TITLE (Include Security Classification)

A Multidriver Shock Tube Model of a Large Blast Simulator

12. PERSONAL AUTHOR(S)
Edmund J. Gion

13a. TYPE OF REPORT Final	13b. TIME COVERED FROM _____ TO _____	14. DATE OF REPORT (Year, Month, Day)	15. PAGE COUNT

16. SUPPLEMENTARY NOTATION

17.	COSATI CODES		18. SUBJECT TERMS (Continue on reverse if necessary and identify by block number)
FIELD	GROUP	SUB-GROUP	Blast Shock Tubes
			Blast Simulators
			Blast Waves

19. ABSTRACT (Continue on reverse if necessary and identify by block number)

The construction of the BRL Multidriver Shock Tube (MD-ST) Model is documented. The facility is a 1:22 model of the Large Blast Simulator at the Centre d'Etude de Gramat, France, except for a lengthened driven tube to permit observation of the full waveform development without interference from the open-end, reflected rarefaction wave (since the Rarefaction Wave Eliminator was not modeled). It is designed with a good safety factor to withstand driver pressures to 24,000 kPa (3,500 psi). Initial tests to greater than 22,100 kPa (3,200 psi) have been performed, and results are compared to other available data. Additionally, the double diaphragm technique, described here, was used to attain the highest shock pressures.

20. DISTRIBUTION / AVAILABILITY OF ABSTRACT ☐ UNCLASSIFIED/UNLIMITED ☒ SAME AS RPT. ☐ DTIC USERS	21. ABSTRACT SECURITY CLASSIFICATION
22a. NAME OF RESPONSIBLE INDIVIDUAL Edmund J. Gion	22b. TELEPHONE (Include Area Code) 301-278-4914	22c. OFFICE SYMBOL SLCBR-TB-B

DD Form 1473, JUN 86   Previous editions are obsolete.   SECURITY CLASSIFICATION OF THIS PAGE

A MULTIDRIVER SHOCK TUBE MODEL

OF A LARGE BLAST SIMULATOR

Edmund J. Gion

ACKNOWLEDGMENTS

CONTENTS

LIST OF FIGURES

LIST OF TABLES

1. INTRODUCTION

This report documents the construction details for the Ballistic Research Laboratory (BRL) Multidriver-Shock-Tube (MD-ST) model of the seven-driver Centre d'Etude de Gramat(CEG), France, Large Blast Simulator (LBS) facility.[1] Assembly and construction details peculiar to the BRL facility were dictated by the exigencies of available pieces and materials and the capability for quick and simple machining procedures.

The construction of the model was deemed a very useful adjunct to the computational efforts on-going within BRL to predict complex shock tube behavior, particularly to support LBS design.[2,3] An axisymmetric Single-Driver-Shock-Tube (SD-ST) model, also scaled to the CEG facility, has produced useful and some otherwise unavailable data for comparison with calculations.[4] However, in view of the proposed U.S. construction of a large multidriver LBS facility (also modeled after the CEG facility), it seemed prudent to assemble a prototype and to perform some tests to assure that performance would be as expected and that unrealized three-dimensional effects were not present.

The following sections illustrate the BRL MD-ST facility construction and present some of the data already obtained. Additionally, an account is given of an operational problem that arose during the tests at the highest shock pressures and how the problem was resolved.

2. FACILITY CONSTRUCTION

2.1 General features. As mentioned, the model for the BRL facility is the operational LBS facility at CEG. A sketch of this facility is shown in Figure 1. The driven tube/test section is noted to be nearly half-cylindrical. Conical nozzles of six-degree half-angle protrude from the seven driver tubes and diaphragm section into the driven tube. A schematic with general overall dimensions is shown in Figure 2 with a cross-sectional view which shows how the nozzles fill out the available driven tube area (~40 percent of full opening). The test station is located seven (effective) driven tube diameters downstream of the nozzle openings. Additionally, for shock pressures above 60 kPa (8.7 psi), the area about the nozzles in the driven tube is left open to the surrounding atmosphere, thereby allowing entrainment of outside air. This procedure permits lengthening the shock wave's positive duration or, in effect, the simulated yield of the blast wave. The seven driver tubes are of four different lengths, as noted in Figure 2, which, on emptying at various times and rates, produce the decaying blast waveform. Examples of the facility's waveforms produced will be seen in the figures to be presented in the "Results" section.

2.2 Driven tube construction. The CEG driven tube shape was, fortuitously, closely duplicatable with existing U-shaped sections from an abandoned modification to the BRL 0.61-m (24-in) shock tube test section. The important dimension for the sections was the half-cylinder
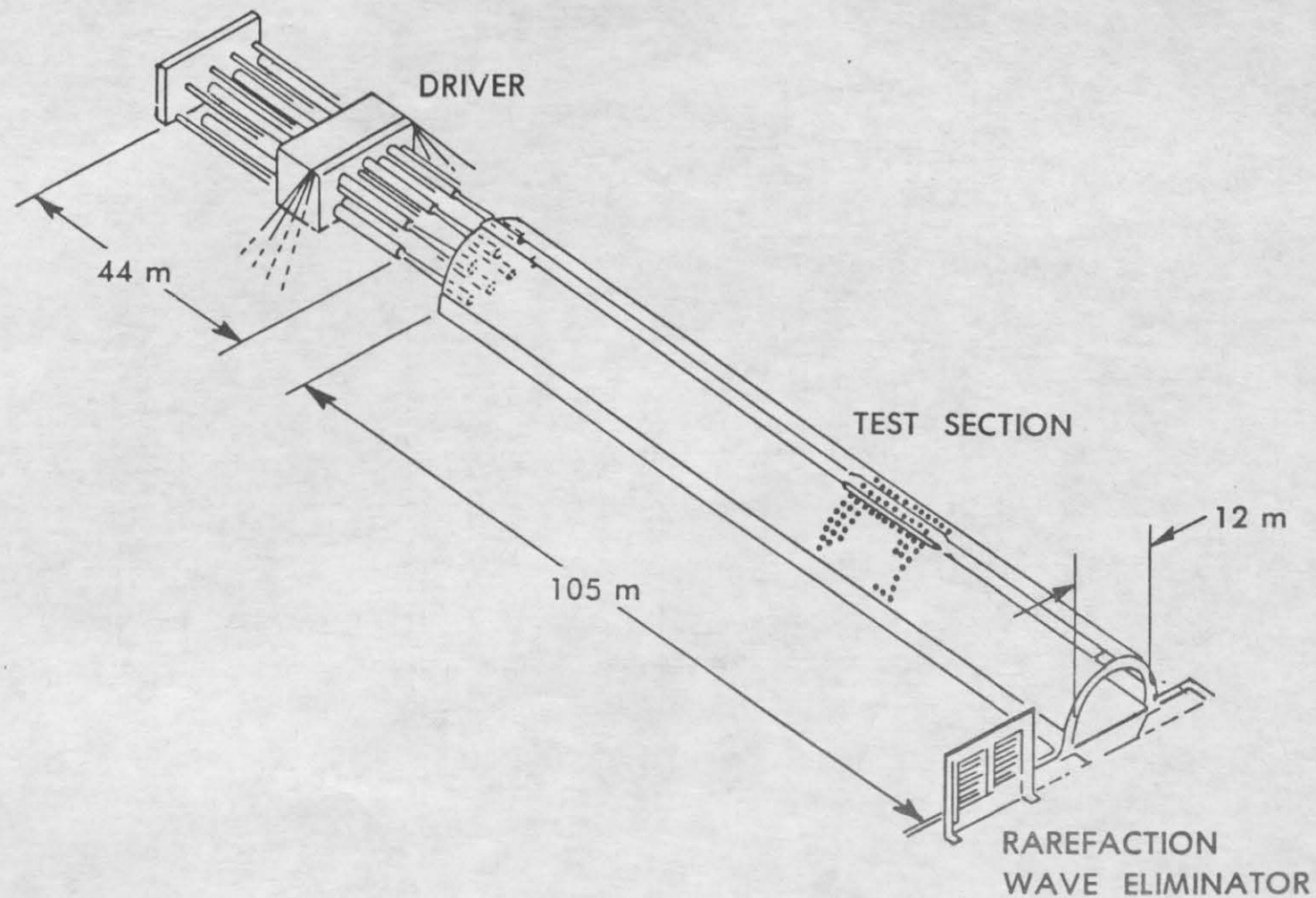
2

BLAST SIMULATOR AT CENTRE d'ETUDES de GRAMAT, FRANCE

Figure 1.   Blast simulator at Centre d'Etude de Gramat, France.

4

9.37 m

1 m

DIAPHRAGM

67.5 m

TEST
STATION

105 m

12 m

1   2   4   6
1   3   5   7

DRIVER NUMBERS AND LENGTHS

$$\left\{\begin{array}{l} 1,7 - 44 \text{ m} \\ 2,6 - 26 \text{ m} \\ 3,5 - 19 \text{ m} \\ 4 - 35 \text{ m} \end{array}\right\}$$
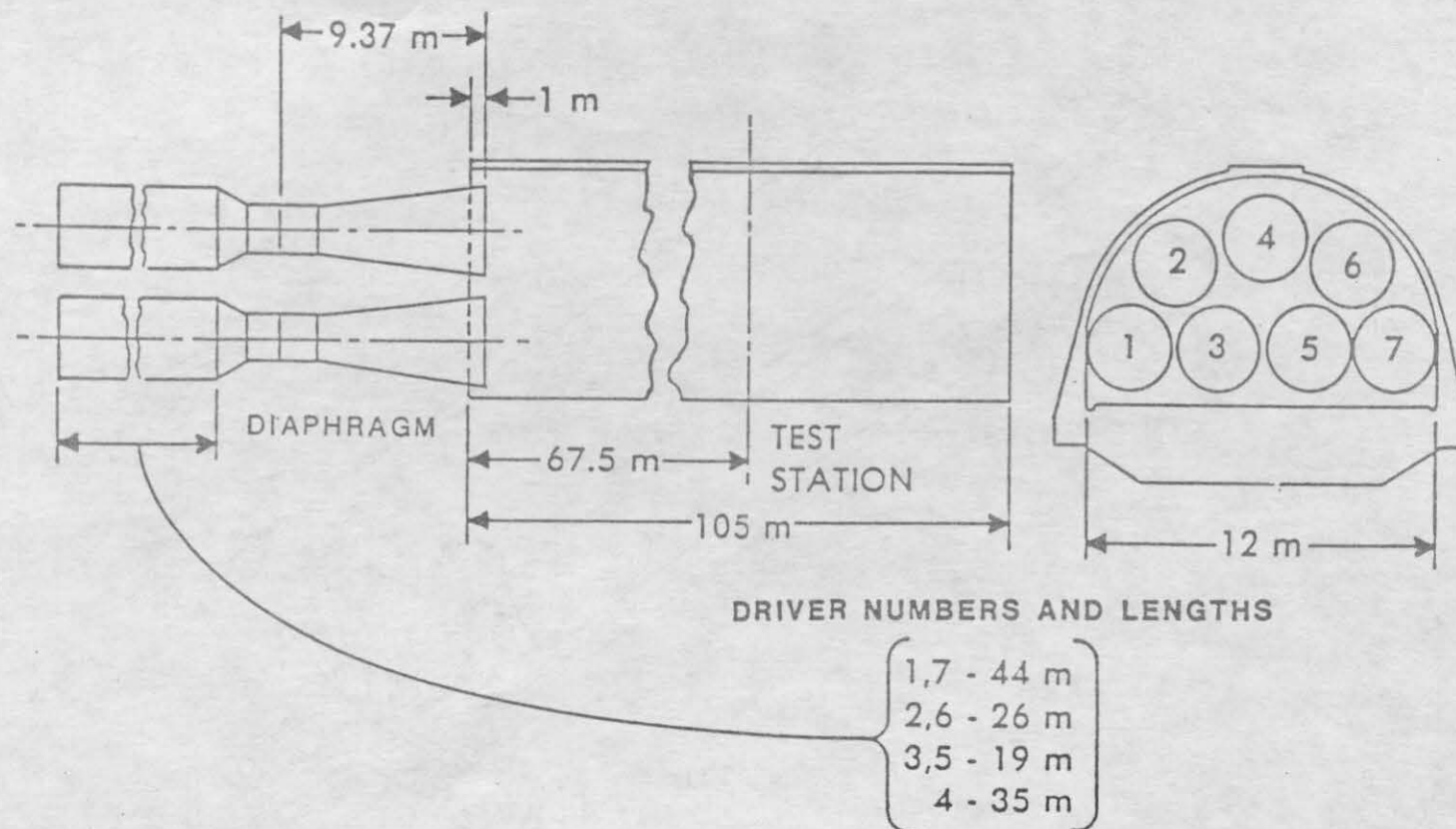
Figure 2.   Important dimensions of CEG large blast simulator.

radius of 0.2873 m (11.312 in) and dictated the length scale for the BRL model--about 1:22 (1:21.58) of the CEG facility. The floor of the driven section is welded in place to a scaled height below the center of the circular cross section, to closely simulate the CEG facility's cross section. In the CEG facility, the vertical walls, at 12 m apart at their floor width, intercept the circular arc of their tube, of radius 6.2 m, at a height of 2.46 m (8.07 ft) above floor level. Our construction leads to a 1.1% greater scaled cross-sectional area than occurs with a true modeling. This should be an insignificant difference, judging from the opposite effect of target blockages in shock tubes being insignificant below about 2%.[5] Heavy metal tabs, welded near the section ends at four places about the periphery, allowed bolting of sections together to form the driven tube length. Extra sections were added, to give a total driven tube length of 13.7 m (45 ft). The extra length over the scaled CEG length was deemed desirable to observe the full waveform development without interference from upstream-running rarefaction waves reflecting from the open end. (The CEG Rarefaction Wave Eliminator was not modeled.) Sealing between section joints was effected by beads of G.E. Silicone RTV caulk placed and pressed into the bolted joint and smoothed on the inside to present a reasonably smooth surface inside the tube. Threaded 1/2"-20 pressure gage ports were made at one- (effective) tube-diameter intervals for the first 10 diameters, then at 2-diameter intervals beyond.

2.3 Driver construction. The driver sections are pieced together from standard seamless steel tubing, using couplers to join tube sections and end plugs and special end pieces to obtain the precise scaled

lengths desired. The main driver tubes are made up of 0.762- and 1.067-m (2-1/2- and 3-1/2-ft) lengths. The short lengths facilitate the boring out required of the stock tubing. Wall thicknesses were chosen to permit driver pressures to 24,000 kPa (3,500 psi) with an estimated safety factor of three. The main tubes have short sleeves, also of stock tubing, welded to their ends and threaded to fit into the couplers. Couplers are likewise of stock steel tubing. An obvious construction note: sleeves should be welded on before threads are turned and ends squared off. Otherwise, the heat may distort the threads, and the weld-bead may find its way into the threads as well. Sealing is effected between the tube sections when the coupler draws up the mating tubing ends, one carrying an O-ring and groove and the other the sealing surface. A thin shoulder in the coupler between the inside threads prevents a tube end from advancing beyond its appropriate thread yet allows for the O-ring sealing. Table 1 lists O-ring sizes and their location, as well as seamless steel tubing used. Table 2 lists geometric features between the CEG and the BRL model facilities.

The high pressure gases for the driver are brought in through the end plugs via thick walled copper tubing. A manifold of four air bottles constitutes the pressurizing system for driver pressures below 13,800 kPa (2,000 psi). For the highest pressures, a secondary bank of three nitrogen bottles is manually switched in and connected to the driver gas tubing. Because of available supplies (or lack of them), the procedure for switching over to the nitrogen supply is the least

6

TABLE 1. Driver Tubing and Details.

			Rough dimension in/m		Machined dimension (OD), in/m
	Tubing	Sched.			
Driver					
	3" nom./ 0.07620m	XX	3.500/0.08890 0.600/0.01524	(OD) (Wall)	3.500/0.08890 2.426/0.6162
Sleeve					
	4" nom./ 0.10160m	160	4.500/0.11430 0.531/0.01349	(OD) (Wall)	4.30/0.1092
Coupling					
	5" nom. 0.12700m	XX	5.563/0.14130 0.750/0.01905	(OD) (Wall)	5.45/0.1384

Note: Location of the O-rings was as follows: Parker #2-120,
diaphragm; Parker #2-140, end plug; Parker #2-147, tubing end.

TABLE 1   Cont.

Driver Tubing Lengths				
		MD-ST Model		CEG
Tube		Make-up	+Endpiece**	
	m in		m in	m
1, 7	2.04 80.3	S*+ 1 L*	0.211 8.3	44
2, 6	1.204 47.4	1 L	0.137 5.4	26
3, 5	0.881 34.7	1 S	0.119 4.7	19
4	1.623 63.9	2 S	0.099 3.9	35

* S = 0.762m/2-1/2ft or 30in

* L = 1.067m/3-1/2ft or 42in

** 0.016m or 5/8in required to accept End Plug

TABLE 2. Geometric Features of CEG and BRL Model Facilities.

	MD-ST model						CEG	
	m	m²	m³	in	in³	ft	m	m²
Driven tube								
Ref. equiv. D	0.442			17.41			9.494	
Cross-section area		0.154	238					70.8
(Semi-circ.) radius	0.2873			11.312			6.2	
Length	13.7					45	105	
Driver tube								
Inside D	0.01661			2.426			1.33	
Throat D	0.03081			1.213			0.665	
Total Volume			0.0295		1,800			

Note: Scale was 21.58 for the MD-ST model and 1 for the CEG model.

satisfactory of the operation. Plans to streamline this part of the operation are being considered. A Bytrex semiconductor pressure gage monitored the pressure in the driver. This is periodically calibrated against a Heise-Bourdon gage.

2.4. Converging-diverging nozzle and diaphragm station.

2.4.1. Converging section. The converging nozzle section is machined from steel bar stock. It has an inlet-to-throat area ratio of 4:1. The section is bolted to a heavy steel reaction pier and caps the lengths of tubing forming a single driver tube. The longer driver tubes are simply supported by a second pier.

2.4.2. Diverging section and diaphragm station. The conical diverging nozzle section is machined from aluminum. Pressure gage ports are provided at the throat section of three of the diverging nozzle pieces and along the wall, at intervals in steps of the throat area. This spacing is thought to be more meaningful for the nozzle flow over spacing equally.

Additionally, nozzles having no diverging section were made up for later shots featuring a discontinuous area change to the driven tube. Earlier shots[6] and other evidence[3] with a single driver shock tube model suggested equivalent performance and better wave shape. Results using these abrupt opening nozzles will be reported at a later date.

An early photograph of the assembled model facility is shown on its mounting stand in Figure 3. The holes in the second mounting pier as placed are not reached by the two shortest driver tubes.

10
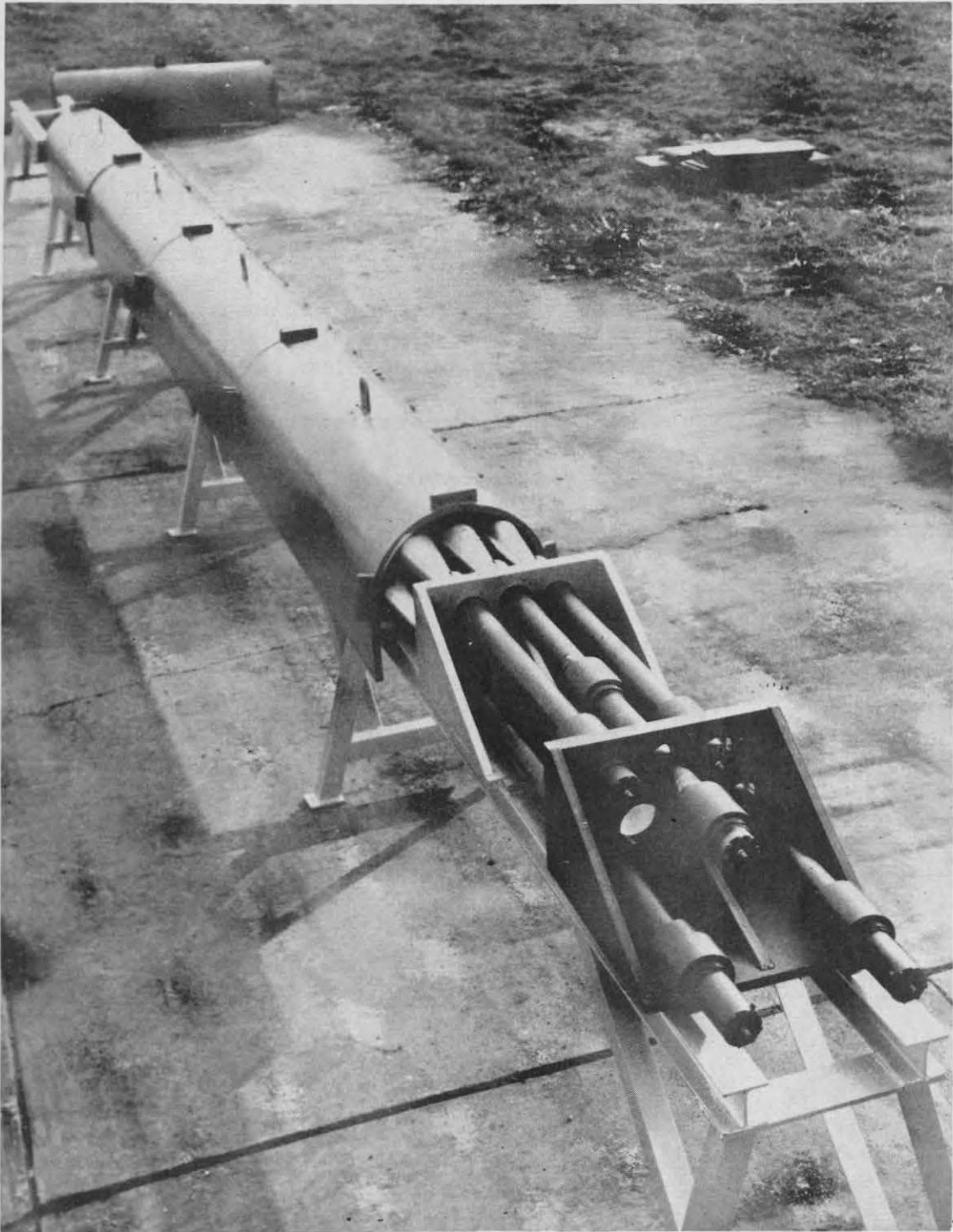
Figure 3. Photograph of BRL multidriver shock tube model.

11

The diaphragm station accepts circular diaphragms, which are cut from various thicknesses of soft, annealed aluminum sheet. The bursting of diaphragms is accomplished with small, exploding bridge wire (EBW) detonators--Reynolds Industries, Inc.; RP-2s containing 20 mg of explosive--which are held against the diaphragm by small wooden sleeves glued to the diaphragm. Diaphragms are pre-bulged to prevent wooden "det-holders" from becoming unglued due to stretching of the aluminum material. For the purpose, a special, small, pre-bulge chamber was made up to allow convenient pre-bulging. Tests in the BRL SD-ST model with a single Reynolds RP-87 detonator (with 68 mg explosive) have demonstrated negligible influence of the detonator blast on the flow.[4] With the MD-ST facility and seven drivers, one has 140 mg explosive using the RP-2s. However, the volume of gas available to be processed by the detonator blast is proportional to $(effect.D)^3$ (since the test station is placed seven effect.D downstream of nozzle openings), which is $(0.442m)^3$ for the MD-ST and $(0.254)^3$ for the SD-ST. The gas volume for the MD-ST is then seen to be greater by a factor 5+. Thus, the detonators' effect on the MD-ST flow may also reasonably be expected to be negligible.

Another problem associated with multiple drivers is simultaneous diaphragm opening. Amann[7] has reported that, for a three-driver shock tube, there are severe distortions of the shock front under circumstances of intentionally delayed diaphragm openings. With electronic control of detonator rupture of diaphragms, it is

12

felt that the diaphragm opening process should be practically sim-
ultaneous for our facility and, hence, not a problem. Additionally,
we have made bench tests of pairs of detonators firing, using the
MD-ST electronics, and photodiode results indicate that the firings
occur within tens of μs of each other. This time interval is a
small fraction of the diaphragm opening time, estimated following an
idealized calculational model[8] to be a few hundreds of μs and,
hence, insignificant.

    2.5. <u>Instrumentation</u>. The instrumentation for the MD-ST model
consists principally of piezoelectric pressure gages placed side-on
in the wall for static pressure measurements, at one or two
(effective) diameters downstream of the nozzle openings, and in
three stagnation pressure rakes of three gages each, mountable at
stations off the tube floor at 2, 3, 7, 9, 12, and 24 diameters from
nozzle openings. Additionally, small, windowed ports were later
provided at 6, 16, and 24 D downstream for small laser beams used to
monitor contact surface passage, supplementing the stagnation pres-
sure probes. The lasers are aimed across the flow at photodiode
sensors, which record a drop in intensity with passage of the vapor
cloud condensed from the cold, expanded air-driver gas.

    The recording of data is via standard analog tape, and data
tapes are digitized and reduced off-line (Fig. 4). Currently, an
effort is being made to change over to digital recording instrumen-
tation for its greater accuracy and convenience, but the changeover
has not yet been accomplished.

13

DATA ACQUISITION SCHEME
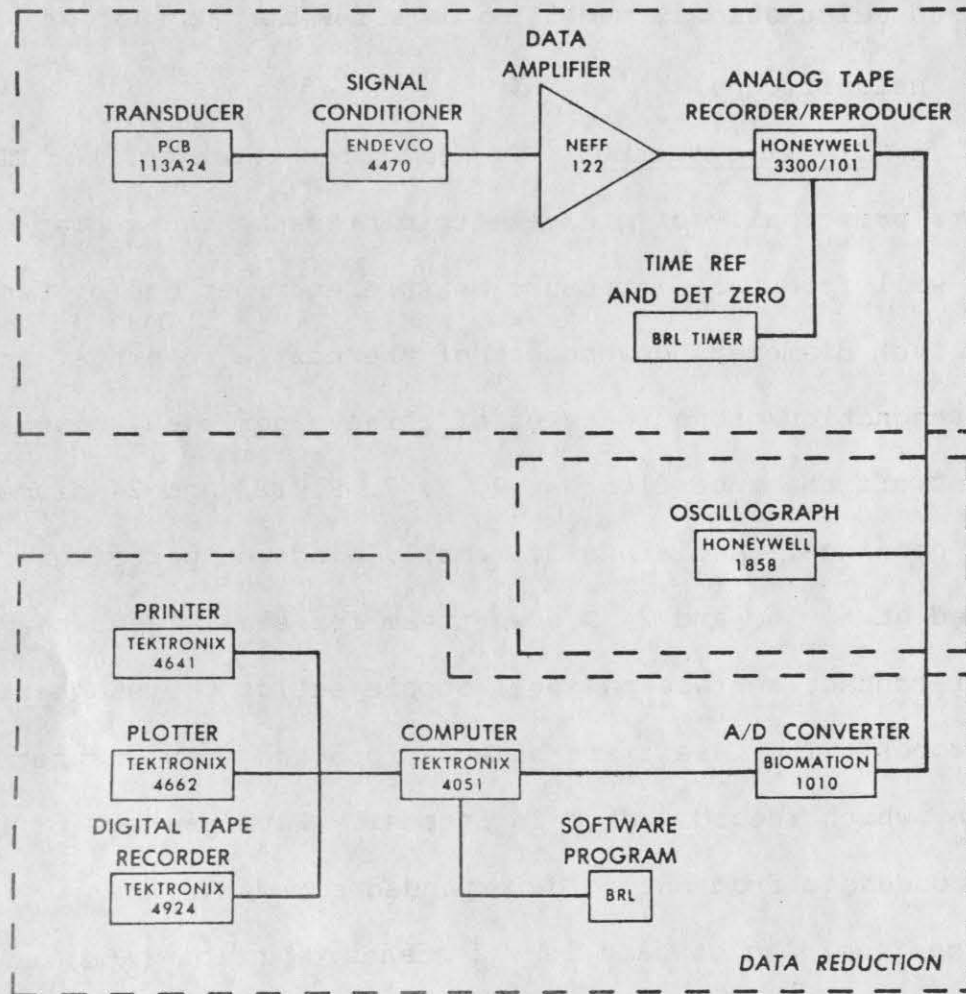
Figure 4. Data acquisition scheme.

14

3.   RESULTS

Sample pressure traces over distances to 14 D downstream of the nozzle are shown in Figure 5 for a mid-level shot--150 kPa (22 psi) at the test station 7.   Station NA1 is located in the nozzle throat, and the trace shows the emptying history of the driver tube.   The pressure waveform takes on the desired decaying blast waveform at the test station 7.   (Station numbers correspond to effective diameters downstream of the nozzle opening.)   Other flow features are noted that have been seen in the axisymmetric SD-ST model and that are discussed there.[4] The noise in the traces in the closer-in stations is believed to be a considerable contribution from the flow disturbances.   These are noted to be much quietened by Station 14 for this run.   The trace of station 7ST is the stagnation pressure trace near the "center" of the tube.   Of particular interest is the pressure spike occurring ~10 ms after shock arrival over the gage. This spike is the cold driver gas flowing over the gage, which complicates proposed drag testing of objects/targets placed in the flow.

A set of runs was performed to prove the performance of the MD-ST model and to provide data to enable comparisons with other data. Table 3 lists the achieved flow conditions and resulting shock pressures.   Additionally, the resulting shock pressure levels for the shots were calculated from measured shock velocities (where available), and these have also been tabulated.   Such data offer assurances of correctness of shock pressures measured beyond problems

15
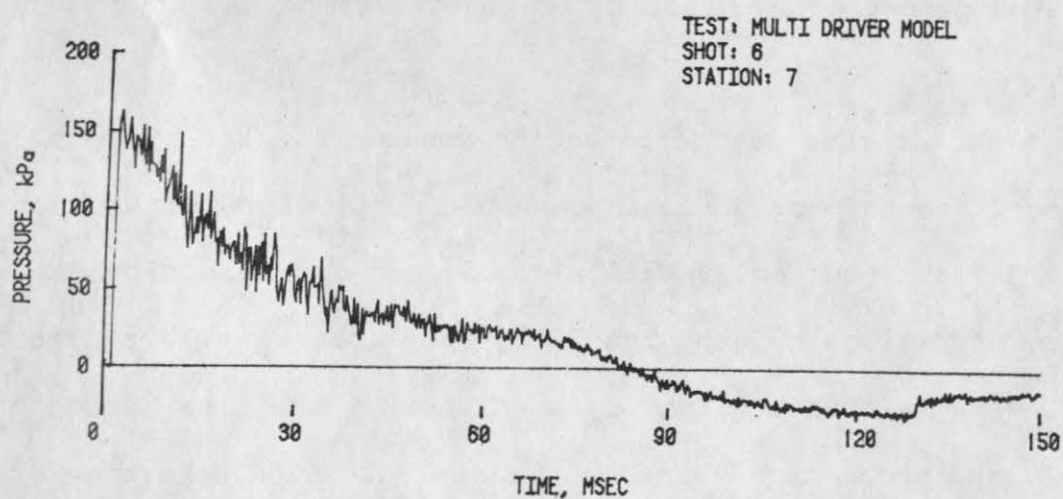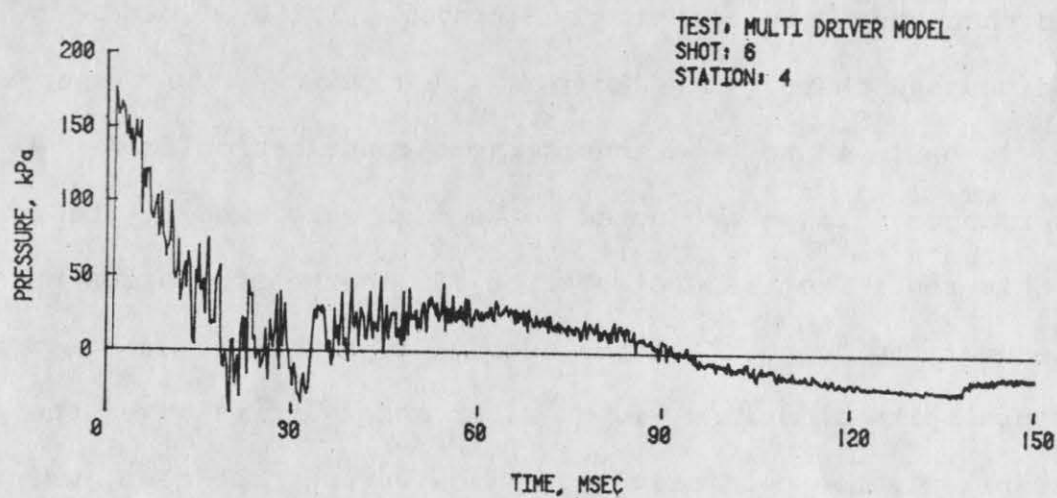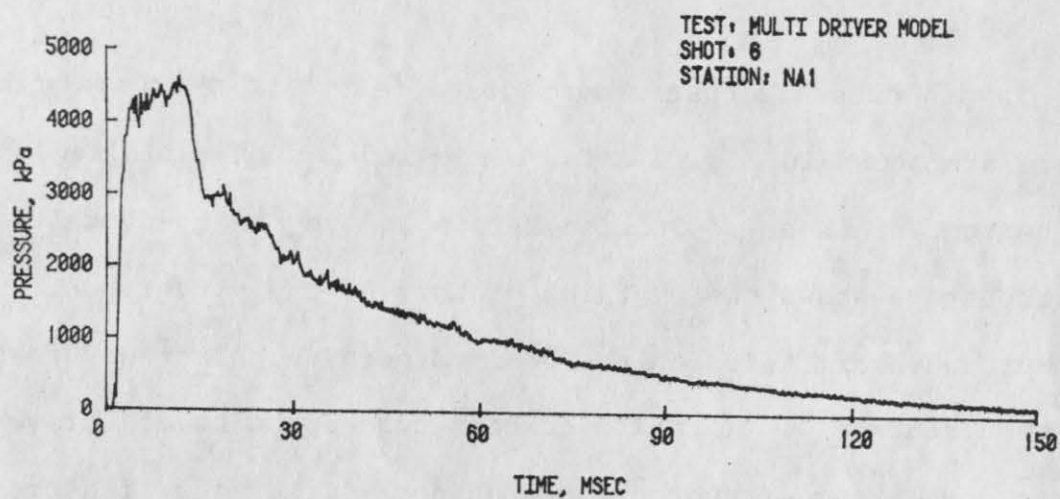
Figure 5. Typical traces for shot in MD-ST model.

TEST: MULTI DRIVER MODEL
SHOT: 6
STATION: 7ST

PRESSURE, kPa (y-axis: 0, 100, 200, 300, 400)
TIME, MSEC (x-axis: 0, 30, 60, 90, 120, 150)

TEST: MULTI DRIVER MODEL
SHOT: 6
STATION: 10

PRESSURE, kPa (y-axis: 0, 50, 100, 150, 200)
TIME, MSEC (x-axis: 0, 30, 60, 90, 120, 150)

TEST: MULTI DRIVER MODEL
SHOT: 6
STATION: 14

PRESSURE, kPa (y-axis: 0, 50, 100, 150, 200)
TIME, MSEC (x-axis: 0, 30, 60, 90, 120, 150)

Figure 5. (Cont.)

17
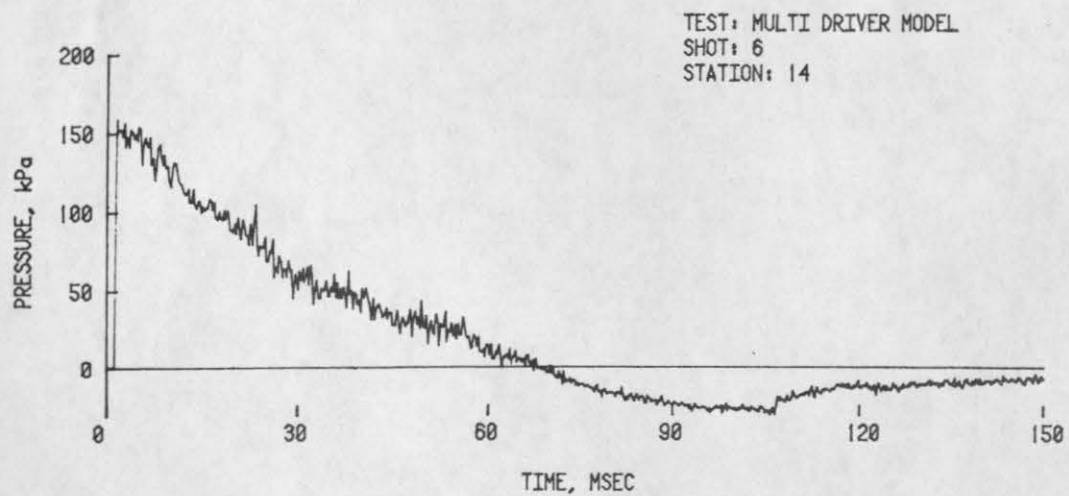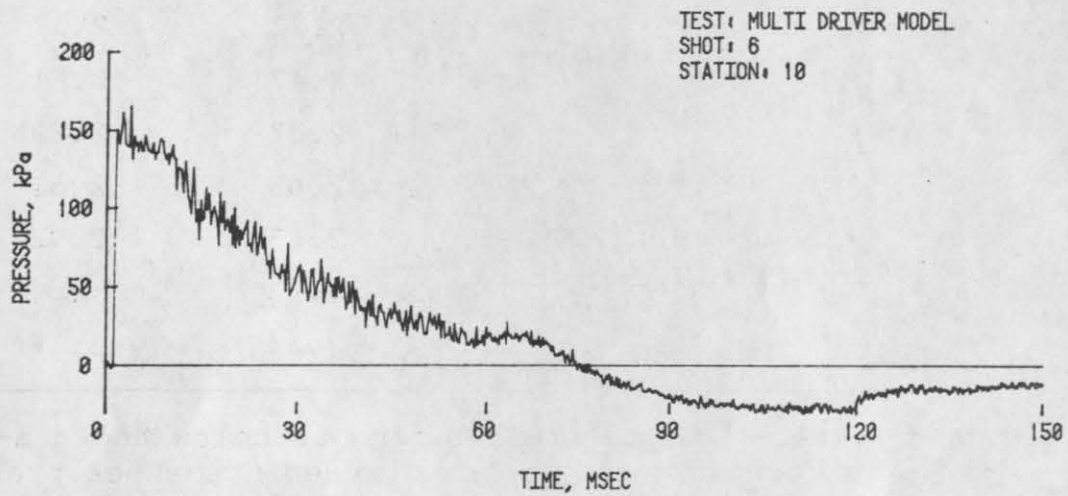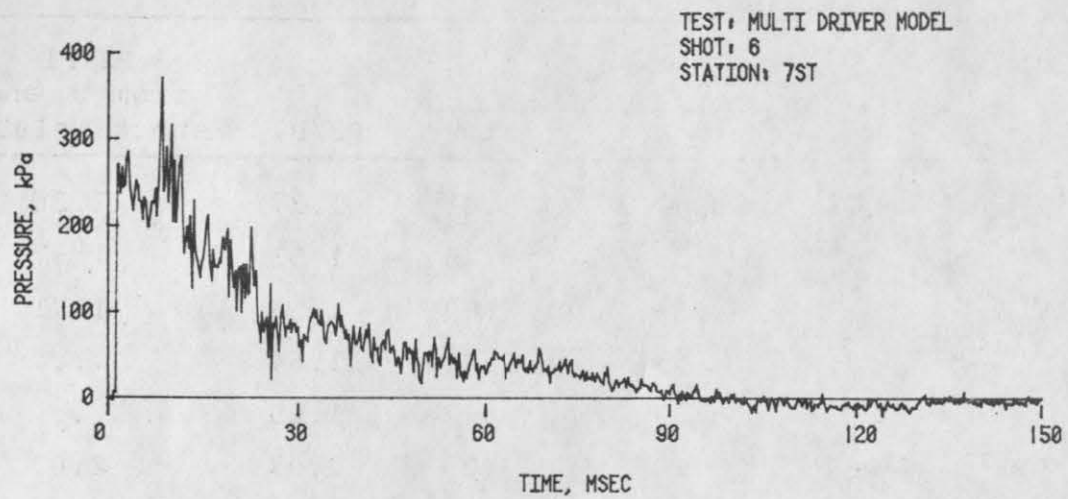
TABLE 3. Multidriver Shock Tube Shots.

| P4/P1 | U_s, m/s | ΔP2 | | P2/P1 | P2/P1 from U_s and shock relations |
		kPa	psi		
17.9	401	37.3	5.41	1.37	1.36
26.4	437	53.4	7.75	1.53	1.67
26.5	447	56	8.09	1.55	1.71
38.2	...	65	9.42	1.64	...
39.7	...	67	9.72	1.65	...
63.1	464	110	16.0	2.07	2.07
64.0	...	105	15.2	2.03	...
81.6	501	125	18.2	2.22	2.37
107.1	524	150	21.8	2.47	2.61
111.0[a]	497	140	20.3	2.37	2.22
128.0	525	170	24.7	2.65	2.51
130.8	538	169	24.5	2.65	2.72
167.0	...	200	29.0	2.93	...
201.0	569	220	32.0	3.14	3.16

[a] A leaking joint limited the pressurizing to below the diaphragm's pre-bulge pressure and, thus, lowered the shock pressure obtained.

18

with gage calibration, imperfect diaphragm rupture, and leaks,

etc. In this regard, we note that, on a few occasions in which

driver pressures were 10-15% below the natural burst pressure for

the diaphragm, the resulting shock pressures tended to be lower

than expected, and the shock's leading edge had a noticeably

slower rise. The lower shock pressures would be confirmed by the

shock velocity calculation.

Figure 6 displays the MD-ST model performance over the range

of shock pressures. The theoretical curve is from a Quasi-1D

calculation.[3] Other data are from the axisymmetric SD-ST model[4]

and from the full-scale facility.[1,9] All of the experimental data

seem to agree reasonably well with each other, and they deviate

from the Q1D calculation at the higher levels, probably due to

non-ideal effects, which are not accounted for in the calcula-

tion.

4. DOUBLE-DIAPHRAGM TECHNIQUE

Reaching the desired shock overpressures of 200+ kPa (30+

psi) required a different procedure. Early on, it was noted that

the thicker diaphragms necessary to hold back the higher pres-

sures were not opening as fully as thought desirable. Indeed, a

shot at a driver pressure of 15,860 kPa (2300 psi) gave a shock

pressure duplicating results at a previous 13,790 kPa (2000 psi)

driver pressure level. Subsequent inspection of burst diaphragms

showed a considerable "necking down" of the diaphragms' open
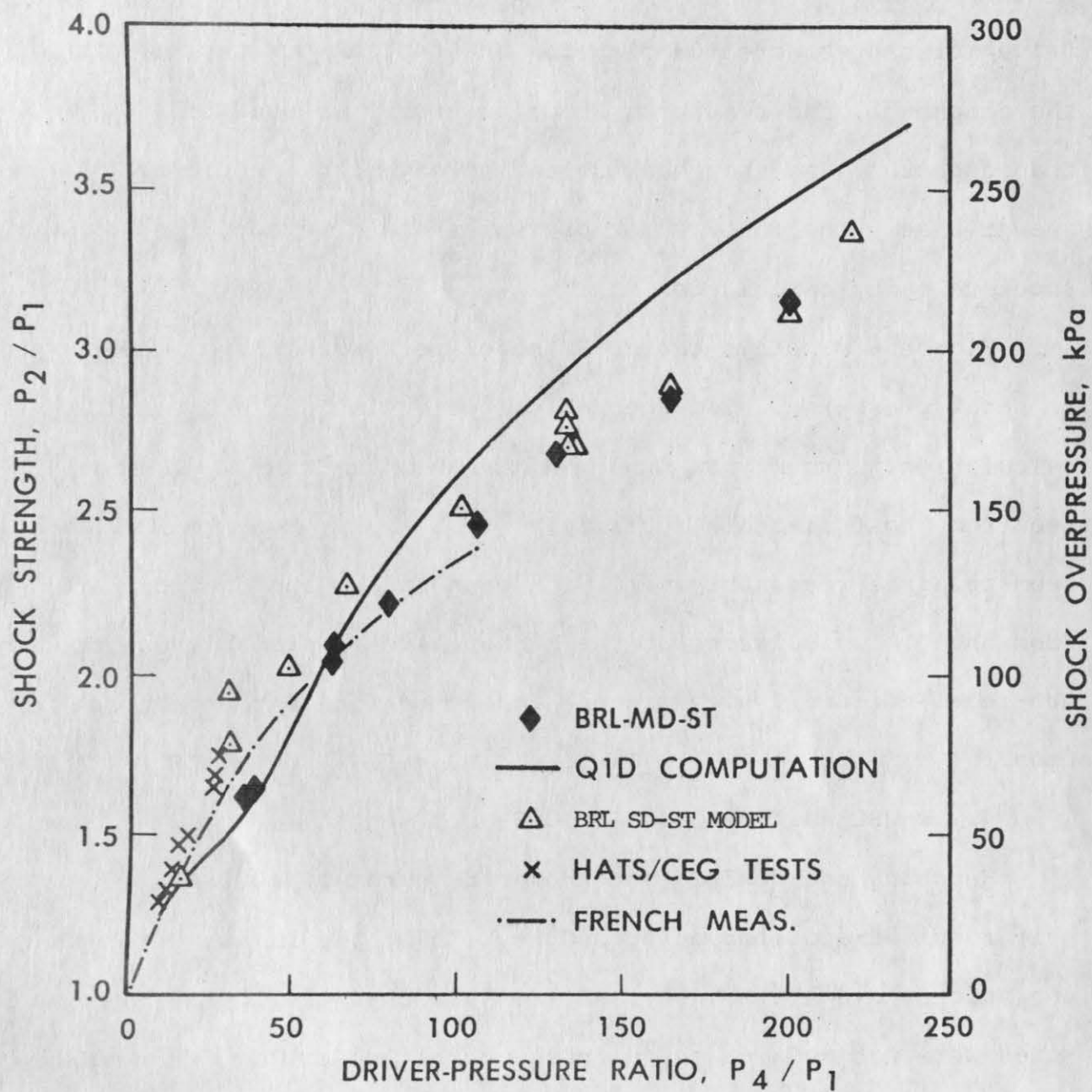
Figure 6. MD-ST model performance and comparisons with other data.

area, thus leading to reduced mass flux and the lower shock pressure. (Shock velocity checks also showed the lower than desired shock flow.) Thoughts of perhaps using larger detonators, scoring of diaphragms, and other diaphragm-opening techniques were considered, but none of these seemed to be the optimal solution.

Attending to the diaphragm seemed to require more knowledge of metals and behavior than was available. Hence, a tactical shift was made to invoke the known technique of using double diaphragms. The procedure would make use of two thinner diaphragms, one diaphragm holding off a reduced pressure, p', which supports the primary diaphragm at the full driver pressure, $p4$, but which needs to hold off only $(p4 - p')$. The intermediate pressure, p', was selected based on previous experience with available diaphragms. This was usually one-half or less of the driver pressure, $p4$, to minimize extraneous wave propagation ahead of the main shock.

To implement the double-diaphragm technique, a set of metal discs were made up, approximately 3.2 cm (1-1/4 in) x 8.25 cm (3.25 in) diameter, appropriately machined for O-ring grooves, and bored to the nozzle throat diameter. Then the two selected diaphragms sealed off and formed the secondary chamber for a disc, which is clamped between converging and diverging nozzle sections. The sketch in Figure 7 shows the double-diaphragm disc

21

AIR INLET

DOUBLE DIAPHRAGM DISC
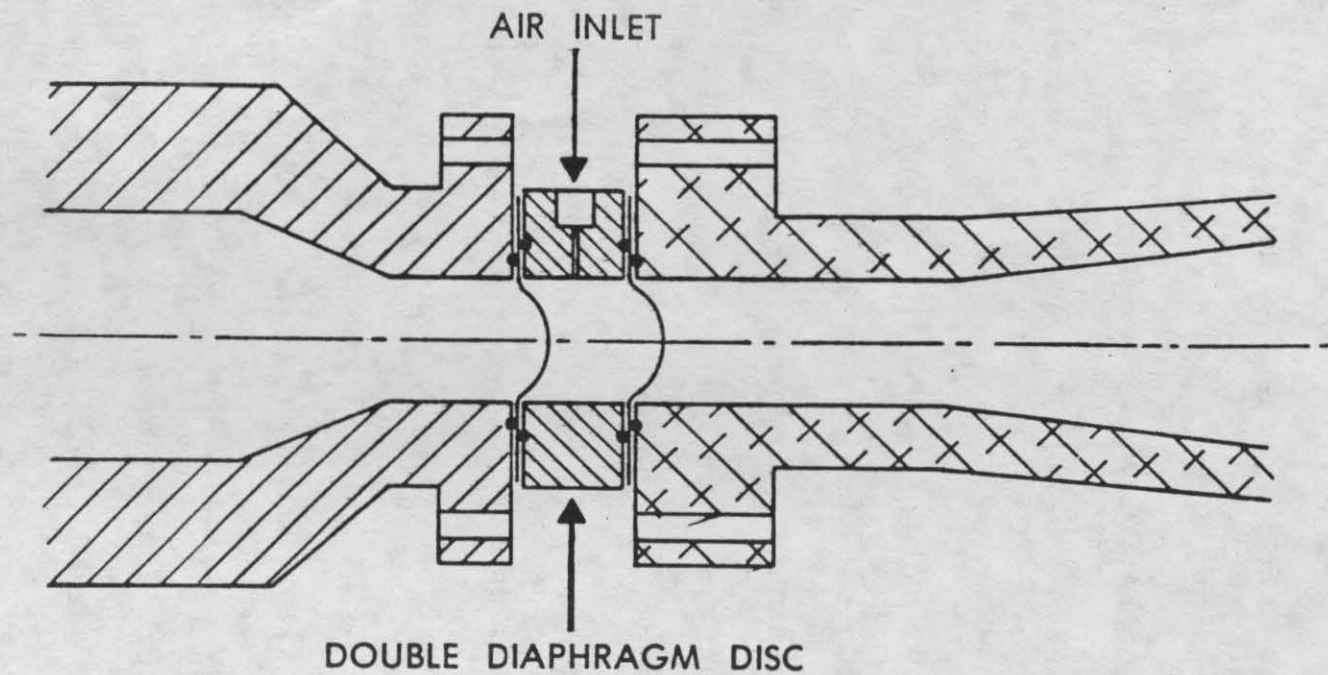
Figure 7.   Implementation of double-diaphragm technique.
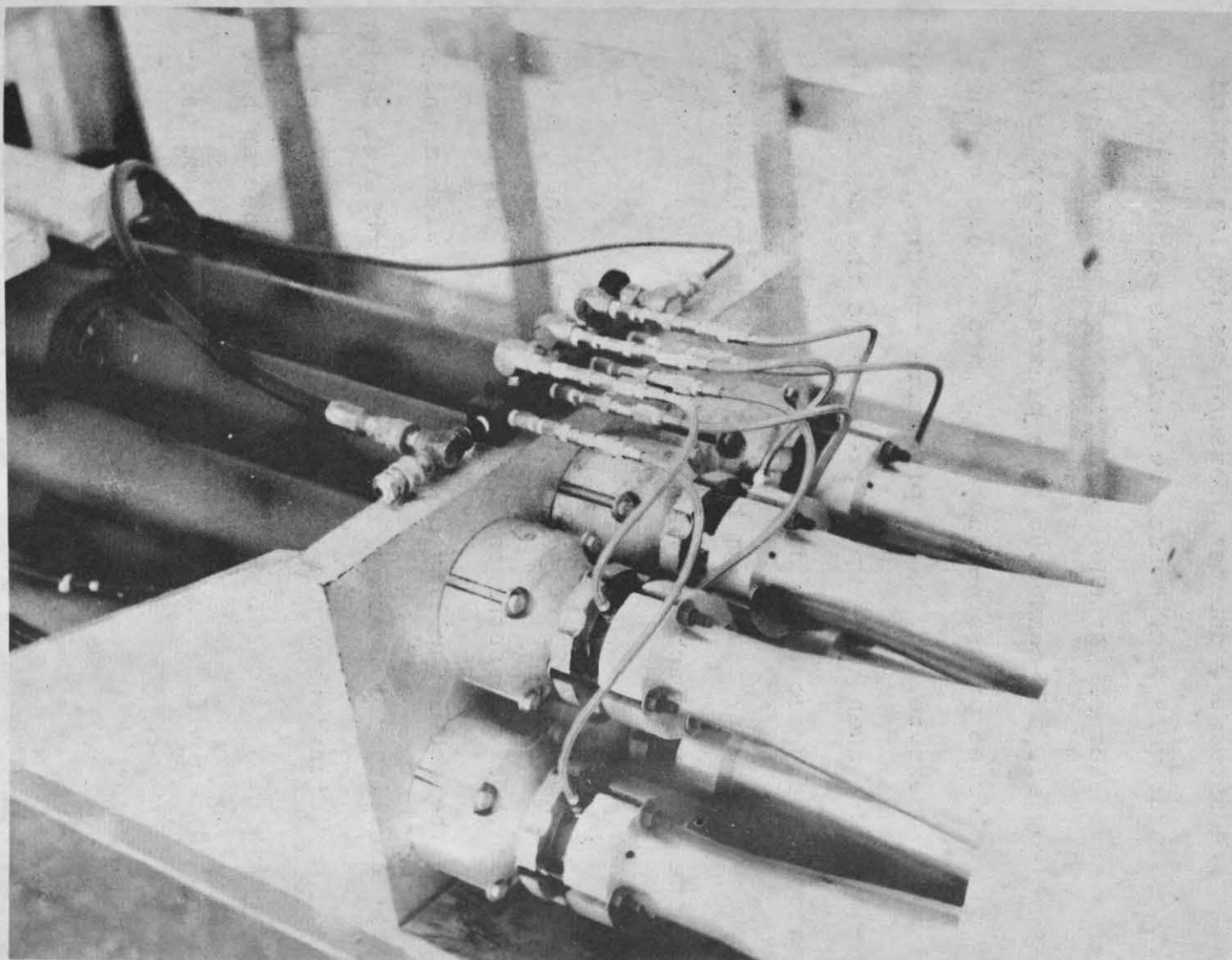
Figure 8.   Photograph of installed double-diaphragm disc
and associated tubing.

23

in position. The photograph in Figure 8 shows the assembled con-
figuration. The secondary chambers are filled from a small mani-
fold block connected by a tube to the primary driver chambers.
In this way, the secondary chamber pressure should lag behind
that in the main drivers and, hence, be less susceptible to
accidental overpressures. At the appropriate p', the secondary
chamber is valved off and connected to a pressure reservoir pre-
filled to the selected pressure--any leaks into or out of the
small volume at pressure, p', cause premature rupture. The main
driver chambers are then taken up in pressure to the desired p4.
The detonators on the secondary diaphragms are then fired,
initiating the secondary diaphragm break, which is followed very
quickly by the primary diaphragm rupture.

5. SUMMARY

Construction of a MD-ST model has been accomplished, and its
performance for shock pressures to 220 kPa (32 psi) has been
demonstrated. The model facility provides the BRL with a unique
experimental facility for testing of Large Blast Simulator design
concepts and modifications and for convenient experimental check
of corresponding flow calculations. Construction features have
been detailed to facilitate the model MD-ST operation and main-
tenance.

6. REFERENCES

1. Gratias, S., and Monzac, J.B.G., "The Large-Scale Nuclear Blast Simulator of the Gramat Research Center: Concept, Research, Performance." Proceedings of the Seventh International Symposium on Military Applications of Blast Simulation, Medicine Hat, Canada, July 13-17, 1981.

2. Pearson, R.J., Opalka, K.O., and Hisley, D.M., "Design Studies of Drivers for the US Large Blast/Thermal Simulator," Proceedings of the Ninth International Symposium on Military Applications of Blast Simulation, AWRE, Foulness, Southend-on-Sea, Essex, England, September 23-27, 1985.

3. Opalka, K.O., and Mark, A., The BRL-Q1D Code: A Tool for the Numerical Simulation of Flows in Shock Tubes with Variable Cross-Sectional Areas, BRL-TR-2763, Ballistic Research Laboratory, Aberdeen Proving Ground, MD, October 1986.

4. Hisley, D.M., Gion, E.J., and Bertrand, B.P., Performance and Predictions for a Large Blast Simulator Model, BRL-TR-2647, Ballistic Research Laboratory, Aberdeen Proving Ground, MD, April 1985.

5. Kingery, C.N., and Bulmash, G., Effects of Shock Tube Blockage on Target Loading, BRL-TR-2689, Ballistic Research Laboratory, Aberdeen Proving Ground, MD, November 1985.

6. Gion, E.J., and Bertrand, B.P., Performance Modifications for an Axisymmetric Large Blast Simulator, BRL-MR-0000, Ballistic Research Laboratory, Aberdeen Proving Ground, MD, to be published.

7. Amann, H.O., "Model Tests for a Large Diameter Simulator Driven by Several Generators Filled with Compressed Air," Proceedings of the Fifth International Symposium on Military Applications of Blast Simulation, Vol. 1, Stockholm, May 23-26, 1977.

8. Drewry, J.E., and Walenta, Z.A., Determination of Diaphragm Opening-Times and Use of Diaphragm Particle Traps in a Hypersonic Shock Tube, UTIAS Technical Note No. 90, University of Toronto Institute for Aerospace Studies, Toronto, June 1965.

9. Teel, G.D., Unpublished data from HATS/CEG tests.

Distribution List

No. of Copies	Organization
12	Administrator Defense Technical Info Center ATTN: DTIC-DDA Cameron Station Alexandria, VA 22304-6145
1	Chairman Department of Defense Explosives Safety Board Hoffman Bldg. 1, Rm 856-C 2461 Eisenhower Avenue Alexandria, VA 22331-0600

1	Office Secretary of Defense
	ADUSDRE (R/AT) (ET)
	ATTN: Mr. J. Persh, Staff
	   Specialist, Materials
	   and Structures
	Washington, DC 20301

1	Under Secretary of Defense for Research and Engineering ATTN: TWP/OM (Hitchcock) Washington, DC 20301-3100
1	Director of Defense Research and Engineering Washington, DC 20301
1	Assistant Secretary of Defense (Atomic Energy) ATTN: Document Control Washington, DC 20301
1	Assistant Secretary of Defense (MRA&L) ATTN: EO&SP Washington, DC 20301
1	Director Defense Advanced Research Projects Agency 1400 Wilson Boulevard Arlington, VA 22209

No. of Copies	Organization
1	Director Defense Intelligence Agency ATTN: DT-1B, Dr. J.Vorona Washington, DC 20301

2	Chairman
	Joint Chiefs of Staff
	ATTN: J-3, Operations
	   J-5, Plans & Policy
	   (R&D Division)
	Washington, DC 20301

3	Director
	Institute for Defense Analyses
	ATTN: Dr. H. Menkes
	   Dr. J. Bengston
	   Tech Info Ofc
	1801 Beauregard St.
	Alexandria, VA 22311

4	Director
	Defense Nuclear Agency
	ATTN: SPTD, Mr.T.E. Kennedy
	   DDST (E), Dr. E. Sevin
	   OALG, Mr. T. P. Jeffers
	   LEEE, Mr. J. Eddy
	Washington, DC 20305

1	Commander Field Command Defense Nuclear Agency ATTN: Tech Lib, FCWS-SC Kirtland AFB, NM 87115
1	HQDA (SARD-TR) Washington, DC 20310-0001
1	HQDA (DAEN-ECE-T/ Mr. R. L. Wright) Washington, DC 20310-0001
1	HQDA (DAEN-MCC-D, Mr. L. Foley) Washington, DC 20310-0001
1	HQDA (DAEN-RDL, Mr. Simonini Washington, DC 20310-0001

Distribution List

Distribution List

29

Distribution List

No. of Copies	Organization
1	Commander Dugway Proving Ground ATTN: STEDP-TO-H, Mr. Miller Dugway, UT 84022
1	Commander US Army Foreign Science and Technology Center ATTN: Research & Data Branch Federal Office Building 220-7th Street, NE Charlottesville, VA 22901
1	Commander US Army Laboratory Command Materials Technology Laboratory ATTN: AMXMR-ATL Watertown, MA 02172-0001
1	Commander US Army Research Office P. O. Box 12211 Research Triangle Park, NC 27709-2211
3	Commander US Army Belvoir Research and Development Center ATTN: STRBE-NN Fort Belvoir, VA 22060-5606
1	Assistant Secretary of the Navy (Research and Development) Navy Development Washington, DC 20350
1	Commander Naval Weapons Center ATTN: Code 0632, Mr. G. Ostermann China Lake, CA 93555
1	Commander Naval Weapons Evaluation Facility ATTN: Document Control Kirtland AFB Albuquerque, NM 87117

No. of Copies	Organization
1	Commander Naval Research Laboratory ATTN: Code 2027, Tech Lib Washington, DC 20375
1	Commander Naval Surface Weapons Center Dahlgren Laboratory ATTN: E-23, Mr. J. J. Walsh Dahlgren, VA 22448
2	Commander Naval Surface Weapons Center White Oak Laboratory ATTN: R-15, Mr. M. M. Swisdak Mr. W. D. Smith III Silver Spring, MD 20902-5000
1	Air Force Systems Command ATTN: IGFG Andrews AFB Washington, DC 20334
3	AFML (LNN, Dr. T. Nicholas; MAS; MBC, Mr. D. Schmidt) Wright-Patterson AFB, OH 45433-6533
1	AFWL/SUL Kirtland AFB, NM 87117-5800
1	Air Force Armament Laboratory ATTN: AFATL/DLODL Eglin AFB, FL 32542-5000
1	Headquarters Department of Energy Office of Military Application Washington, DC 20545
1	Mr. Richard W. Watson Director, Pittsburgh Mining & Safety Research Center Bureau of Mine, Dept of the Interior 4800 Forbes Avenue Pittsburgh, PA 15213

Distribution List

31

Distribution List

No. of Copies	Organization	No. of Copies	Organization
1	J. G. Engineering Research Associate 3831 Menlo Drive Baltimore, MD 21215	1	Science Applications, Inc. Suite 310 1216 Jefferson Davis Highway Arlington, VA 22202
1	McDonnell Douglas Astronautics Western Division ATTN: Dr. Lea Cohen 5301 Bosla Avenue Huntington Beach, CA 92647	2	Battelle Memorial Institute ATTN: Dr. L. E. Hulbert Mr. J. E. Backofen, Jr. 505 King Avenue Columbus, OH 43201
1	Physics International 2700 Merced Street San Leandro, CA 94577	1	Georgia Institute of Tech ATTN: Dr. S. Atluri 225 North Avenue, NW Atlanta, GA 30332
1	R&D Associates ATTN: G. P. Ganong P. O. Box 9335 Albuquerque, NM 87119	1	IIT Research Institute ATTN: Mrs. H. Napadensky 10 West 35 Street Chicago, IL 60616
2	The Boeing Company Aerospace Division ATTN: Dr. Peter Grafton Dr. D. Strome Mail Stop 8C-68 P. O. Box 3707 Seattle, WA 98124	2	Southwest Research Institute ATTN: Dr. H. N. Abramson Dr. U. S. Lindholm 8500 Culebra Road San Antonio, TX 78228
2	AVCO Corporation Structures and Mechanics Dept. ATTN: Dr. William Broding Dr. J. Gilmore 201 Lowell Street Wilmington, MA 01887	1	Brown University Division of Engineering ATTN: Prof. R. Clifton Providence, RI 02912
1	Aerospace Corporation P. O. Box 92957 Los Angeles, CA 90009	1	Florida Atlantic University Dept. of Ocean Engineering ATTN: Prof. K. K. Stevens Boca Raton, FL 33432
1	General American Transportation Corp General American Research Div. ATTN: Dr. J. C. Shang 7449 N. Natchez Avenue Niles, IL 60648	1	Texas A&M University Department of Aerospace Engineering ATTN: Dr. James A. Stricklin College Station, TX 77843
1	Lovelace Research Institute ATTN: Dr. E. R. Fletcher P. O. Box 5890 Albuquerque, NM 87115	1	University of Alabama ATTN: Dr. T. L. Cost P. O. Box 2908 University, AL 35486

Aberdeen Proving Ground

Dir, USAMSAA
ATTN: AMXSY-D
      AMXSY-MP, H. Cohen
Cdr, USATECOM
ATTN: AMSTE-TO-F
Cdr, CRDEC, AMCCOM
ATTN: SMCCR-RSP-A
      SMCCR-MU
      SMCCR-SPS-IL
Cdr, US Army Toxic and
Hazardous Materials Agency
ATTN: AMXTH-TE